UV-visible Spectra and Gas-Phase Rate Coefficients for the Reaction of 2,3 pentanedione and 2,4-pentanedione with OH Radicals

L. Messaadia, G. El Dib, Azeddine Ferhati, Abdel Chakir

UV-visible Spectra and Gas-Phase Rate Coefficients for the Reaction of 2,3-pentanedione and 2,4-pentanedione with OH Radicals

L. MESSAADIA[1,2], G. El DIB[3], A. FERHATI[2] and A. CHAKIR[4*]

[1]Faculté des Sciences Exactes et Informatique Département de Chimie Université de Mohamed Seddik Ben Yahia B.P: 98 Ouled Aissa Jijle 18000 Algeria

[2]*Laboratoire LCCE, Faculté des sciences, Université de Batna, rue Boukhlouf El Hadi 05000 Batna , Algeria*

[3] *Institut de Physique de Rennes, UMR 6251 du CNRS - Universite´ de Rennes 1, Bat. 11c, Campus de Beaulieu, 35042 Rennes Cedex, France*

[4]*GSMA-UMR CNRS 7331, UFR Sciences, université Reims Champagne Ardenne BP 1039, 51687 Reims cedex 02,France*

ABSTRACT

The UV absorption cross-sections of 2,3-pentanedione and 2,4-pentanedione were measured and their reactions with OH were investigated in the gas-phase using a relative rate method. A temperature dependence of the rate coefficients was observed for both reactions over the temperature range 298 -338 K. This work provides the first UV cross-section in the gas phase for 2,4-pentanedione and the first kinetic data for the reaction of 2,3-pentanedione with OH radicals as a function of temperature. The tropospheric lifetimes obtained in this work suggest that once emitted into the atmosphere, these species could be quickly degraded close to their emission sources.

Keywords: 2,3-pentanedione ; 2,4-pentanedione; Hydroxyl radical; UV spectra; rate coefficient; Kinetics; Atmospheric Chemistry.

* Corresponding author : E mail address : abdel.chakir@univ-reims.fr

Phone number: 0033 3 26913263

1. Introduction

Diketones are a variety of Volatile Organic Compounds (VOCs) which contain two keto carbonyl groups (C=O). These species are used in several industrial applications. For example α-dicarbonyls compounds are used as solvents [1] and starting materials for the organic compounds synthesis. Due to their Keto−Enol tautomerization, β-diketones are widely used in several industrial sectors, mainly in the preparation of chelate compounds [2]. In addition to these emission sources, these compounds can be formed in situ in the atmosphere through the oxidation of anthropogenically emitted VOCs [3]. As other VOCs, these species are removed from the atmosphere, by photolysis and by reactions with the atmospheric oxidants such as OH radicals leading to the formation of other secondary pollutants [4].

Although the atmospheric photooxidation of C_2-dicarbonyls (glyoxal) and C_4 (biacetyl) has been described in several studies [5, 6], few data exist on ≥ C_5-diketones atmospheric degradation.

The purpose of this work was to measure the UV-visible absorption spectra of two C_5-diketones and to study their kinetics with OH radicals as a function of temperature. The studied compounds were: 2,3-pentanedione (α-diketone) and 2,4-pentanedione (β-diketone).

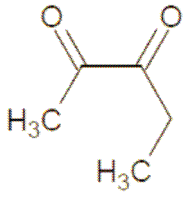

2,3-pentanedione

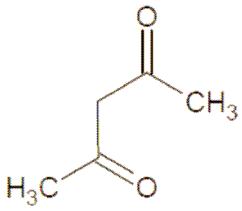

2,4-pentanedione

To our knowledge, only one kinetic study is available in the literature on α diketones. In fact, recently, Szabo et al.[7] have studied the photolysis and the kinetics of 2,3-pentanedione with OH radicals. The kinetic measurements were carried out using both absolute and relative methods at room temperature. A recommended value of $(2.09 \pm 0.40) \times 10^{-12}$ cm^3 $molecule^{-1}s^{-1}$ was reported by these authors at 300 K. In addition, the UV absorption cross sections for 2,3-pentanedione were determined in the same work over the spectral range of 220 to 450 nm. The obtained UV spectrum was found to be shifted compared to that determined previously by Jackson et al., [8] mainly at short wavelengths. In addition, the maximum of cross sections obtained in this spectral region by Szabo et al.,[7] was found to be lower by a factor of 2 than that measured by reference [8].

2,4-pentanedione could be in the keto and enol forms at the same time in solution but, in the gas phase, the enol form is most favourable (90%). Only three kinetic studies on 2,4-pentanedione are found in the literature [9,10,11]. However, no data exist on the UV absorption cross sections of 2,4-pentanedione. Dagaut et al. [9] have studied the gas phase reactions of a series of cyclic ketones and diones including butanedione, 2,4-pentanedione and 2,5-hexanedione with the OH radicals at room temperature. The kinetic study was carried out by using an absolute rate method based on the flash photolysis-resonance fluorescence technique. A value of $(1.15 \pm 0.15) \times 10^{-12}$ cm^3 $molecule^{-1}$ s^{-1} was obtained for 2,4-pentanedione. In the study carried out by Holloway et al. [10], 2,4-pentanedione was used as a precursor for OH radicals. The kinetics of the reaction of OH with 2,4-pentanedione was investigated by these authors in the gas-phase using two different techniques. An average value of $(8.78\pm0.58)\times10^{-11}$ $cm^3molecule^{-1}s^{-1}$ was reported by these authors. This rate coefficient is almost two orders of magnitude higher than that previously reported by Dagaut et al., [9]. In the study carried out by Zhou et al., [11], a kinetic study on the reactions of 2,4-pentanedione with OH and ozone has been performed in a 1080 L quartz glass reaction chamber using in situ FTIR spectroscopy analysis. Rate coefficients with OH were determined over the temperature range of 285 to 310 K. A value close to that obtained by Holloway et al. [10] of $(9.05\pm1.81)\times10^{-11}$ cm^3 $molecule^{-1}s^{-1}$ was obtained at 298 K.

In order to more assess the removal processes of diketones in the atmosphere by chemical reactions and by photolysis, further laboratory studies are required. In fact, the evaluation of the photolysis and OH reaction contribution to the atmospheric removal of $\geq C_5$ diketones requires accurate knowledge of their UV-visible spectra, photolysis rates and rate coefficient for reaction with OH. Besides to the atmospheric interest, the spectroscopic data are very useful in the detection and quantification of the studied species in several reactive systems and photochemical studies.

The present work provides the first kinetic data for the reaction of 2,3-pentanedione with OH radicals as a function of temperature and the first UV absorption cross sections in the gas phase for 2,4-pentanedione. In addition, in this work, kinetic data for the reaction of 2,4-pentanedione with OH and the UV spectrum of 2,3-pentanedione are measured and reported in this work. The obtained data are used to estimate the effective lifetimes in the troposphere of the studied compounds.

2. Experimental section

2.1. UV-visible spectrum

The experimental setup used to measure the UV cross sections of 2,3-pentanedione and 2,4-pentanedione has been previously described [12,13], therefore, it will only be described briefly here. The light source consists of a 30 W deuterium lamp as a source of UV and a tungsten lamp as a source of visible radiation. A lens is used to focus the light into a spectrometer (HR 640) equipped with a 2400 line mm^{-1} grating (dispersion 0.66 $nm.mm^{-1}$ for HR 640). At the exit slit of the monochromator, the beam passes through the absorption pyrex cell. The signal is measured by a Hamamatsu R 955 photomultiplier tube. The width of the entrance slit was varied from 80 to 200 μm yielding a spectral resolution ranging from 0.05 to 0.20 nm. The vapours of the purified compounds were introduced under vacuum into the absorption cell, equipped with quartz optical windows. In order to measure the absorption with good accuracy, two absorption Pyrex cells of different lengths were employed: the first one is 50 cm in length and 2.5 cm in diameter and the second one is 160 cm in length and 2 cm in diameter.

Platinum resistance temperature sensors positioned at the extremities of each cell were used to provide continuous and simultaneous temperature readings. Meanwhile, the pressure inside the cells was measured by (0 – 100) Torr MKS Baratron capacitance manometers. Before each experiment, the spectrophotometer background noise $I_n(\lambda)$ and the intensity of the issued radiation $I_0(\lambda)$ were measured under vacuum in the absence of the studied compounds and in the same spectral region. The transmitted intensity $I(\lambda)$ is measured at each wavelength in the presence of the studied compounds. Pressures were measured at the beginning and the end of each measurement to check for the stability of the concentration of the introduced sample.

The absorption cross-section (σ_λ) values were determined using the Lambert-Beer's law (1), as a function of the pressure P, temperature T, optical path l and intensities described above. R represents the gas constant and N_A is Avogadro's number.

$$\sigma_\lambda = \ln\left(\frac{I_0(\lambda) - I_n(\lambda)}{I(\lambda) - I_n(\lambda)}\right) \times \frac{R.T}{P.l.N_A} \qquad (1)$$

The concentrations introduced in the absorption cell and the path lengths were chosen in such way so as to obtain optical density values between 0.1 and 2, conditions for which the cross-section is determined with good accuracy. Before every experiment, the residual

background noise of the spectrometer was measured. At the end of each run, the cell was pumped and purged with He and $I_o(\lambda)$ was recorded to check the stability of the light source during a sequence of measurements. The experimental conditions used during these measurements are summarized in Table 1.

2.2. Reactions with OH radicals

The reactions of 2,3-pentanedione and 2,4-pentanedione with OH radicals were studied using an atmospheric simulation chamber coupled to a FTIR spectrometer. The experimental set-up has been previously described [14], therefore, it will only be described briefly here. The reactor is a triple-jacket pyrex cell (length 2 m, internal diameter 20 cm) equipped with a multiple reflection system. The first two outer layers of the chamber delimit a vacuum in order to isolate the whole system from its surroundings. The temperature regulation is provided by water circulating between the inner wall and the second jacket using a thermostat (Julabo FPW 90) operating in the temperature range of 25 to +100 °C. Platinum resistance temperature sensors were used to provide continuous and simultaneous temperature readings. The pressure inside the cell was measured by (0 – 1000) Torr MKS Baratron capacitance manometers. An Equinox 55 FT-IR spectrometer was used to monitor the consumption of the reactants and reference compounds. The spectral resolution was in the range of 2-0.5 cm^{-1} in the spectral range of 600 to 4000 cm^{-1}. 24 UV lamps symmetrically arranged emitting from 300 to 400 nm were used to generate OH by the photolysis of nitrous acid which was produced in a drop-wise by the addition of 10 % of sulphuric acid to a solution of 0.2 M of sodium nitrite. A small flow of nitrogen gas was used to carry the generated nitrous acid into the reactor. In this work, benzaldehyde and 2-methyl 3-buten-2-ol were used as reference compounds. The reference compounds were chosen in such a way that at least one absorption band of the studied compound does not exhibit any interference with those of the studied diketones and vice versa. Measured amounts of reagents were flushed from calibrated bulbs into the reactor through a stream of ultra-pure air. The reactor was then filled at atmospheric pressure with ultra-pure air. The experimental conditions used for the kinetic study are summarized in Table 1.

The measurements were performed in purified air provided by Air Liquide (> 99.9999%). The used reagents: benzaldehyde (99.5%), 2-methyl-3-buten-2-ol (98%), 2,3-pentanedione (97%) and 2,4-pentanedione (99.5%) were provided by Sigma-Aldrich. They were further purified by distillation and by repeated freeze-pump-thaw cycles before use in both the spectroscopic and kinetic studies.

3. Results and Discussion

3.1. UV-visible spectrum

Absorption was measured in a series of (50 - 100 nm) adjacent regions with a 10 nm overlap. Using equation (1), cross-sections were calculated after each measurement. The absorption spectra are illustrated in Figure 1 and the cross sections in Table 2.

General characteristics of the obtained spectra*:* As can be seen in Figure 1, the obtained spectra consist of a broad continuum. Both spectra exhibit no fine structures. Globally, the absorption between 210-340 nm for 2,3-pentanedione was found to be less than that of 2,4-pentanedione. The spectrum of 2,3-pentanedione shows two absorption bands attributed to the n-π* forbidden electronic transitions due to the presence of two carbonyl groups. The first band is located between 225 and 300 nm, and the second one is located between 325 and 470 nm. In addition to these two absorption bands, a third one, attributed to the $\pi \rightarrow \pi^*$ electronic transition of the carbonyl chromophore, was observed below 210 nm. The absorption UV spectrum of 2,3-pentanedione determined in this work exhibits a similar shape as that of butanedione [15] in terms of the band positions and widths.

For 2,4-pentanedione, a large absorption band located between 210 and 340 nm was observed showing a maximum located around 262 nm ($\sigma_{max} = 4{,}5\times10^{-17}$ $cm^2molecule^{-1}$). This molecule exists in two isomeric forms: Keto and Enol forms. Both forms have an absorption band between 250 and 290 nm as seen in the study carried out by Bernasconi and Kanavarioti, [16] where the UV spectrum of 2,4 –pentanedione in solution has been determined. In the *Keto* form, the absorption is weak and is due to a n-π* forbidden electronic transition. Whereas, in the *Enol* form, the high absorption is attributed to the $\pi \rightarrow \pi^*$ electronic transition of an unsaturated α,β-ketone, and the less intense absorption is attributed to a n-π* forbidden electronic transition. As mentioned before, in the gas phase, this molecule most favourably (90%) exits in the Enol form which may be the source of the intense absorption band.

Sources of errors: The studied compounds were introduced into the cell at pressures less that their vapor pressures at room temperature in order to minimise errors due to the loss on the walls. The error on the cross section values, due to the pressure measurements and the purity degree of the studied compounds is estimated to 10%. Other sources of error (less than 1%) include the wavelength calibration, the temperature instability and the optical length. Each cross section value reported in Table 2 is the average of 3 to 8 independent measurements at several pressures, so that statistical uncertainties would be minimized. In fact, for 2,3-pentanedione, the variation between experiments does not exceed 5% and 15%

over the spectral ranges 200-310 nm and 310-450 nm, respectively; this variation increases in the other spectral ranges but does not exceed 25%. For 2,4-pentanedione, variations of 10% below 315 nm and 25% above 315 nm were found.

Comparison with previous studies: To the best of our knowledge, there is no published study of the UV–visible absorption spectra of 2,4-pentanedione in the gas phase. However, two studies are found in the literature concerning the UV spectrum of 2,3-pentanedione [7,8]. Jackson et al. [8] reported the UV absorption spectrum of 2,3-pentanedione measured at room temperature by using a monochromator with a spectral resolution of 0.6 nm coupled to photomultiplier. As can be seen in Figure 2, the general shape of the spectrum obtained in this work is similar to that obtained by Jackson et al. [8]. In addition, the cross sections obtained in the present work are in good agreement (less than 20%) with those obtained by reference [8] in the spectral range 270-460 nm. However, outside this spectral region, discrepancies between our values and those obtained by Jackson et al., 1972 vary from 20 to 80%.

The UV spectrum of 2,3-pentanedione was also measured by Szabo et al. [7] under static and dynamic conditions at room temperature by using a D_2 lamp-coupled to a monochromator with a spectral resolution of 0.4 nm. The comparison shows that the absorption bands obtained by these authors are shifted, to longer wavelength (10 nm) for the first band and to shorter wavelength for the second one, compared to the spectra obtained in this work and by Jackson et al. [8]. In addition, the second band located around 420 nm, obtained in this work, was found to be larger than that obtained by Szabo et al. [7]. In the spectral range of 270 to 420 nm, a discrepancy less than 20% is found between our values and those obtained by Szabo et al. [7]. However, this discrepancy reaches 40% in other spectral regions, most probably due to the shift in wavelength.

3.2 Reactions with OH radicals

The rate coefficients of the following reactions were measured:

OH + 2,3-pentanedione → products (1) $k_{2,3\text{-pentanedione}}$ at (301-338 K)

OH + 2,4-pentanedione → products (2) $k_{2,4\text{-pentanedione}}$ at (298-333 K)

The rate coefficients of the reactions of OH radicals with the reference compounds used in this study are (in $cm^3 molecule^{-1} s^{-1}$):

$k_{(benzaldehyde+OH))} = 5.33\times10^{-12}\, e^{((242.9\pm85)/T)}$ ([17])

$k_{(2\text{-methyl-3-buten-2-ol+OH})} = 8.2\times10^{-12}\, e^{((609.8\pm 49)/T)}$ ([18])

The rate coefficients of the reactions of the studied diketones with OH were obtained using the following relation:

$$\frac{1}{t-t_0}\times\ln\left(\frac{[diketone]_t}{[diketone]_{t0}}\right)=\frac{\left(k_{diketone}/k_{ref}\right)}{t-t_0}\times\ln\left(\frac{[ref]_t}{[ref]_{t0}}\right)+\left(\left(k_{diketone}/k_{ref}\right)\times k_p'-k_p\right) \quad (2)$$

where $[diketone]_0$ and $[ref]_0$ are the initial concentrations of the studied diketone and the reference compound, respectively; $[diketone]_t$ and $[ref]_t$ are the concentrations of the studied diketone and the reference compound at time t. $k_{diketone}$ and k_{ref} are the rate coefficients of the reactions of OH with the studied diketone and the reference compound, respectively. k_p and k'_p are the global rate coefficients due to the loss of the studied diketones and the references compounds, respectively, by secondary processes (photolysis, wall losses).

Figures 3a-3b represent the plots of $\frac{1}{t}\ln\left(\frac{[diketone]_0}{[diketone]_t}\right)$ vs $\frac{1}{t}\ln\left(\frac{[ref]_0}{[ref]_t}\right)$ according to equation (2) where the initial time is equal to zero and the consumption of studied compound due to secondary processes is taken into account . These plots are straight lines with the slope equal to $\frac{k_{diketone}}{k_{ref}}$. In both figures, good linearity is observed with a correlation coefficient greater than 90%. The obtained rate coefficients are summarized in Table 3. The overall uncertainties on the rate coefficient values reported in Table 3 include both statistical errors due to the fit and systematic errors due to the experimental conditions and the error on k_{ref} (20 - 30 % according to the used reference compound, as reported in the literature). In the temperature range explored in this work, a dependence of the rate coefficient on the temperature was observed for the reactions of OH with 2,3-pentanedione and 2,4-pentanedione. A linear least-squares analysis of the data yielded the activation energy and the preexponential factor. The following temperature dependent expressions of the rate coefficients (cm^3 $molecule^{-1}$ s^{-1}) were as follows:

$k_{2,3\text{-pentanedione + OH}}(T) = (1.06 \pm 0.15) \times 10^{-10} e^{((-1052 \pm 160)/T)}$ (301-338 K)

$k_{2,4\text{-pentanedione + OH}}(T) = (5.20 \pm 0.60) \times 10^{-12} e^{((824 \pm 30)/T)}$ (298-333 K)

Temperature effect : The rate coefficient shows a positive temperature dependence for the reaction of OH with 2,3-pentanedione. Whereas, the rate coefficients for the reaction of OH

with 2,4-pentanedione determined in this work exhibit a strong negative temperature dependence. Our results agree with those reported by Zhou et al.[11] and suggest that this reaction is dominated by the addition of OH on the C=C double bond of 2,4-pentanedione predominantly in the Enol form in the gas phase.

Comparison with previous studies: The study of the gas-phase atmospheric chemistry of 2,3-pentanedione with OH radicals is presently limited to only one investigation [7]. The absolute and relative-rate kinetic values reported by Szabo et al. [7] are in good agreement with each other and a recommended rate coefficient of $(2.09 \pm 0.40)\times10^{-12}$ cm^3 $molecule^{-1}$ s^{-1} is reported at 300 K. Our value obtained at 301 K at atmospheric pressure is higher than this value by a factor of 1.5 although the error bars of the present work overlap with those found by Szabo et al. [7]. The origin of the discrepancy may be due to systematic errors coming from the experimental techniques and from the reference compounds used in both studies. To our knowledge, no kinetic data are reported in the literature for the reaction of 2,3-pentanedione with OH as a function of temperature.

The reaction of 2,4-pentanedione with OH radicals has been investigated in three previous studies [9,10,11]. The comparison with the values reported in the literature for the reaction of 2,4-pentanedione with OH, shows that no difference is observed between our value $(8.76 \pm 2.70)\times10^{-11}$ and the average value reported by Holloway et al. [10] at room temperature. A very good agreement is found between our values and those obtained by Zhou et al. [11]. However, our value is almost two orders of magnitude higher than that reported by Dagaut et al. In their study, Dagaut et al. generated OH from the UV photolysis of H_2O at $\lambda \geq 165$ nm. As mentioned in Section 3.1 and as seen in Figure 1, 2,4-pentanedione exhibits high absorption in the UV region which could lead to its photodissociation. This may be an additional source of OH radicals during the experiments, that could distort the decay of OH due to its reaction with 2,4-pentanedione. In addition, as stated by Holloway et al. [10], the reaction may be in the fall off region over the pressure range of 25 to 50 Torr used during the study carried out by Dagaut et al. [9].

Effect of the structure on the reactivity: As for other aliphatic ketones, the reaction of 2,3-pentanedione with OH radicals is expected to proceed mainly by H-abstraction process from the C-H bonds. The reactivity of 2,3-pentanedione with OH studied in the present work is compared to that of butanedione ($CH_3C(O)C(O)CH_3$). Our value is 1 order of magnitude higher than that reported for butanedione by Dagaut et al. [9] $(2.3\pm0.2)\times10^{-13}$ cm^3 $molecule^{-1}s^{-1}$ which is in very good agreement with that reported by Darnall et al. [19]. This comparison

shows that the reactivity of these species with OH increases with increasing carbon chain. This increase in the reactivity is due to the presence of the hydrogen atoms linked to the carbon atoms located in a β-position with respect to the CO group [20,21]. In addition hydrogen atoms that are attached to secondary carbons are the most likely attack sites [22-23]. As explained in references [24-25] reactivity enhancement of the C-H bond at the β position is due to the formation of a cyclic intermediate complex which tends to significantly reduce the activation energy barrier.

The reactivity of OH with 2,4-pentanedione, a β-diketone molecule was found to be 29 times higher than that obtained for 2,3-pentanedione in the present work. This increase in reactivity shows that the reaction of OH with 2,4-pentanedione is dominated by a fast addition of OH radicals on the C=C double bond, present the Enol form of 2,4-pentanedione.

4. Atmospheric implications

4. 1 Atmospheric photodissociation rate constants:

The obtained cross-sections are used to estimate the photolysis rates of the studied diketones. Such estimation may be used to assess the importance of photolysis as a degradation process, even in the absence of direct photolysis studies under atmospheric conditions. Averaged photodissociation rate constants (J_p) were calculated using the following relationship:

$$J_p = \int \sigma(\lambda)\, \phi(\lambda)\, I(\lambda)\, d\lambda \quad (\text{III})$$

where $\sigma(\lambda)$ is the absorption cross-section at wavelength λ (cm^2 $molecule^{-1}$), $\phi(\lambda)$ is the primary quantum yield of photodissociation at wavelength λ, and $I(\lambda)$ is the actinic flux of the solar radiation at wavelength λ (photons cm^{-2} s^{-1}).

J_p values were calculated for different zenith angles θ varying from 20° to 50° at 40°N latitude corresponding to the morning of a cloudless day (Table 4). The actinic flux values at sea level were taken from Demerjian et al. [26]. J_p values for 2,3-pentanedione were calculated using the global quantum yield of 0.2 recently determined by Bouzidi et al. [27]. A quantum yield of unity was used to calculate those for 2,4-pentendione since the overall quantum yield for this species is not known (Table 4). Photolysis rates of the same order of magnitude were obtained for both compounds. These rates are relatively high due to the fact that 2,4-pentanedione has a strong absorption in the range 290-340 nm and 2,3-pentanedione absorbs over the entire spectral range 350-470 nm.

4. 2 Tropospheric lifetime calculations

The tropospheric lifetimes due to reactions with atmospheric oxidants were estimated according to the equation $\tau = 1/k[X]$ where [*X*] represents the average concentration of the atmospheric oxidant and *k* the rate coefficient for the reaction of the studied diketone with the oxidant. The rate coefficient obtained in this work was combined with the average tropospheric concentration of OH radicals to estimate the tropospheric lifetimes of the studied diketones due to their reaction with OH. In addition, the lifetimes of the studied compounds due to photolysis were calculated by using photolysis rate constants J_p determined in this work (Table 4). It should be noted that the photolysis rate are higher limits while photolysis lifetimes are lower limits.

In Table 5, the lifetimes of 2,3-pentanedione and 2,4-pentanedione due to the OH reactions and photolysis and calculated in this work are compared to those due to their reactions with other atmospheric oxidants (Cl and O_3). The lifetimes were calculated by using an average global tropospheric concentration of 1×10^6 molecule cm^{-3} [28] and 1×10^3 molecule cm^{-3} [29] for OH radicals and Cl atoms respectively.

The reactivity of 2,3-pentanedione towards Cl atoms was investigated by Kaiser et al.[3] and a rate coefficient of $(1.4\pm0.3)10^{-11}$ $cm^3molecule^{-1}s^{-1}$ was obtained. Zhou et al. [11] studied the reaction of 2,4-pentanedione with O_3 and calculated a value of 16.1 days for the lifetime of this compound due to its reaction with O_3, assuming an average tropospheric concentration (in molecules cm^{-3}) of ozone of 7×10^{11}.

The lifetimes of 2,3-pentanedione and 2,4-pentanedione obtained in this work indicate that photolysis and the gas-phase reaction with the OH radicals are the main loss process for these species in the atmosphere. However, the reactions with Cl atoms could be an important loss process for these species in coastal areas where the concentration of Cl atoms reaches 1×10^5 molecule cm^{-3} [30].

5. Conclusion

This work provides the first UV-Visible absorption cross sections in the gas phase for 2,4-pentanedione. A very intense absorption band was observed for 2,4-pentanedione in the 210-340 nm spectral range showing the dominance of the enol form for this molecule in the gas phase. For 2,3-pentanedione two absorption bands were observed in the 210-500 nm spectral range.

This work provides the first determination of the rate coefficient of the reaction of OH radicals with 2,3-pentanedione as a function of temperature. A positive temperature dependence was obtained for 2,3-pentanedione and a negative temperature dependence was observed for 2,4- pentanedione due to the OH addition on the C=C bound present in the Enol form of this molecule. The comparison of the reactivity of 2,3-pentanedione, 2,4-pentanedione and butanedione shows that the molecular structure of these compounds may have an impact on the reactivity of these species.

Data obtained in this work allowed us to estimate the atmospheric lifetime of these compounds with respect to photolysis and degradation by reaction with OH. The lifetimes of these species are relatively short suggesting that the presence of these compounds in the atmosphere may generate a photochemical pollution mainly at the local scale.

Acknowledgements

The authors gratefully thank the INSU-LEFE program for financing this study.

References

[1] Burdock, G.B.; Fenarolli's Handbook of Flavor Ingredients, 5th ed.; CRC Press: Boca Raton, FL, 2005.
[2] Yoon, M.C.; Chio, Y. S.; Kim, S. K. *J. Chem. Phys*. **1999**, 110, 11850–11855.
[3] Kaiser, M.; Wallington T. J.; Hurley M. D. *The Journal of Physical Chemistry A* , **2010**, 114, 343–354.
[4] Finlayson-Pitts, B. and Pitts, J.N., 'Chemistry of the upper and lower atmosphere: theory, experiments, and applications'; 2000, New York, Academic Press.
[5] Tadic, J.; Moortgat,G.K.; Wirtz, K. *J. Photochem. Photobiol., A*, **2006**, 177, 116.
[6] Rajakumar, B.; Gierczak, T.; Flad, J.E.; Ravishankara, A.R.; Burkholder, J.B *J. Photochem. Photobiol. A*, **2008**, 199, 336.
[7] Szabo, E.; Djehiche, M.; Riva, M.; Fittschen, C.; Coddeville, P.; Sarzynski, D.; Tomas, A.; Dobé, D. *J. Phys. Chem A.,* **2011**, 115, 9160-9168.
[8] Jackson, A. W.; Yarwood, A. J. *Canad. J. Chem.*, **1972**, 50, 1331-1337.
[9] Dagaut, P.; Wallington, T.J.; Liu, R.; Kurylo, M.J. *Phys. Chem.,* **1988**, 92, 4375-4377.
[10] Holloway, A. L.; Treacy, J.; Sidebottom, H. W.; Mellouki, A.; Daële, V.; Le Bras, G.; Barnes, I. *J. Photobiol. and Biochem. A. Chem.,* **2005**, 176, 183-190.
[11] Zhou, S.; Barnes, I.; Zhu, T.; Bejan, I.; Albu, M.; Benter, T. *Environm. Sc. and Tech.*, **2008**, 42, 7905-7910.
[12] Chakir, A.; Solignac, G.; Mellouki, A.; Daumont, D. *Chem.Phys.Lett.*, **2005**, 404, 74-78.
[13] Messaadia, L.; El Dib, G.; Ferhati, A.; Roth, E.; Chakir, A. *Chem.Phys. lett.*, **2012**, 529, 6 - 22.
[14] Messaadia, L.; El Dib, G.; Klendar, M.; Cazaunau, M.; Roth, E.; Ferhati, A.; Mellouki, A.; Chakir, A. *Atmospheric Environment*, **2013**, 77, 951-958.
[15] Horowitz, A.; Meller, R.; Moortgat, G. K. J. *Photochem. Photobiol.,A* **2001**, 146, 19.
[16] Bernasconi and Kanavarioti, *J.Am. Chem. Soc*., **1986** 108, 7744-7751.
[17] Semadeni, M.; Stocker, D.W.; Kerr, J.A. *Int. J. Chem. Kin.*, **1995**, 27, 287-304.

[18] Rudich, Y.; Talukdar, R.; Burkholder, J.B.; Ravishankara, A.R. *J. Phys. Chem*, **1995**, 99, 12188-12194.
[19] Darnall, K.; Atkinson, R.; Pitts, J. N. *J. Phys. Chem*. **1979**, 83, 1943-1946.
[20] Wallington, T. J.; Kurylo, M. J. *J. Phys. Chem*. **1987**, 91, 5050.
[21] Mellouki, A.; Le Bras, G.; Sidebottom, H. *Chem. Reviews,* **2003**, 103, 5077.
[22] Atkinson, R.; Aschmann, S. M. *J. Phys. Chem*. **1988**, 92, 4008.
[23] Atkinson, R.; Aschmann, S. M. *Int. J. Chem. Kinet*. **1995**, 27, 261.
[24] Atkinson, R. D.; Baulch, L.; Cox, R. A.; Hampson, R. F., Jr.; Kerr, J. A.; Rossi, M. J.; Troe, J. *J. Phys. Chem. Ref. Data*, **1999**, 28, 191.
[25] Alvarez-Idaboy, J.R.; Cruz-Torres, A. ; Galano, A.; Ruiz-Santoyo, M.E. J. *Phys. Chem. A*, **2004**, 108, 2740-2749.
[26] K.L. Demerjian, K.L. Schere, J.T. Peterson, Adv. Environ. Sci. Tech. 10 (1980) 369.
[27] Bouzidi H.; Fittschen C.; Coddeville P.; Tomas A. *Atmos Env*, **2014**, 82, 250-257
[28] Atkinson, R.; Baulch, D.L.; Cox, R.A.; Hampson, R.F.; Kerr, J.A.; Rossi, M.J.; Troe, J. *J. phys. and Chem. Ref. data*, **1997**, 26, 1329 – 1499.
[29] Wingenter, O. W.; Blake, D. R.; Blake, N. J.; Sive, B. C.; Rowland, F. S.; Atlas, E.; Flocke, F. *J.Geophys.Res-Atmos.* **1999**, *104*, 21819 - 21828.
[30] Spicer, C.W.; Chapman, E.G.; Finlayson-Pitts, B.J.; Plastridge, R.A.; Hubbe, J.M.; Fast, J.D.; Berkowitz, C.M.; *Nature*, **1998**, 394, 353–356.

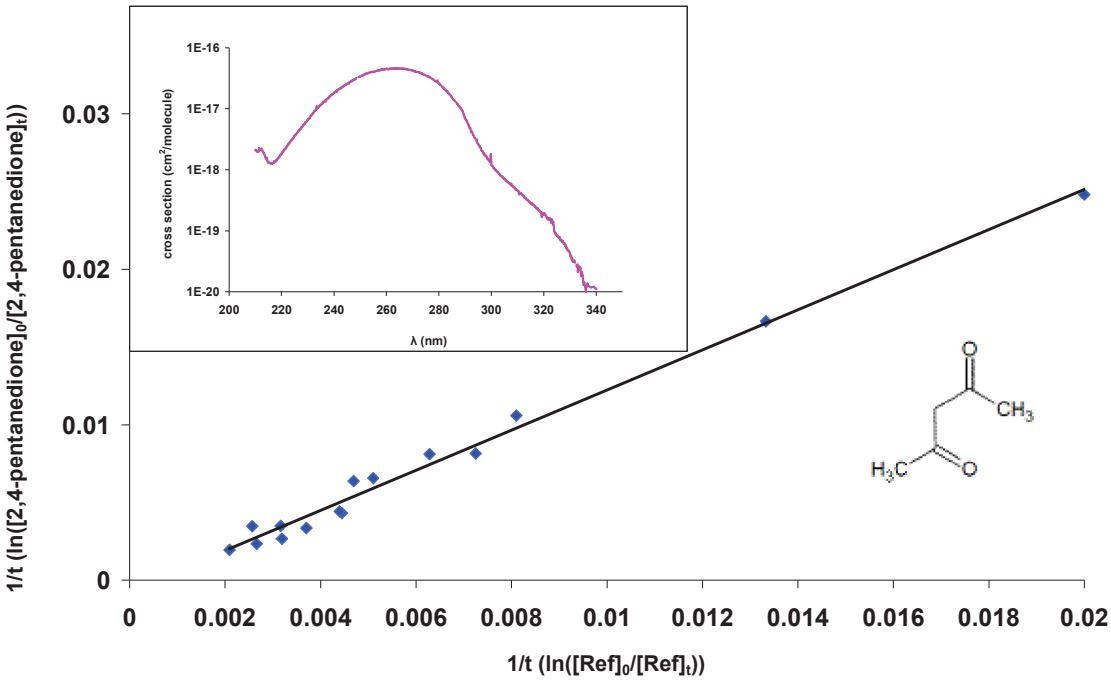

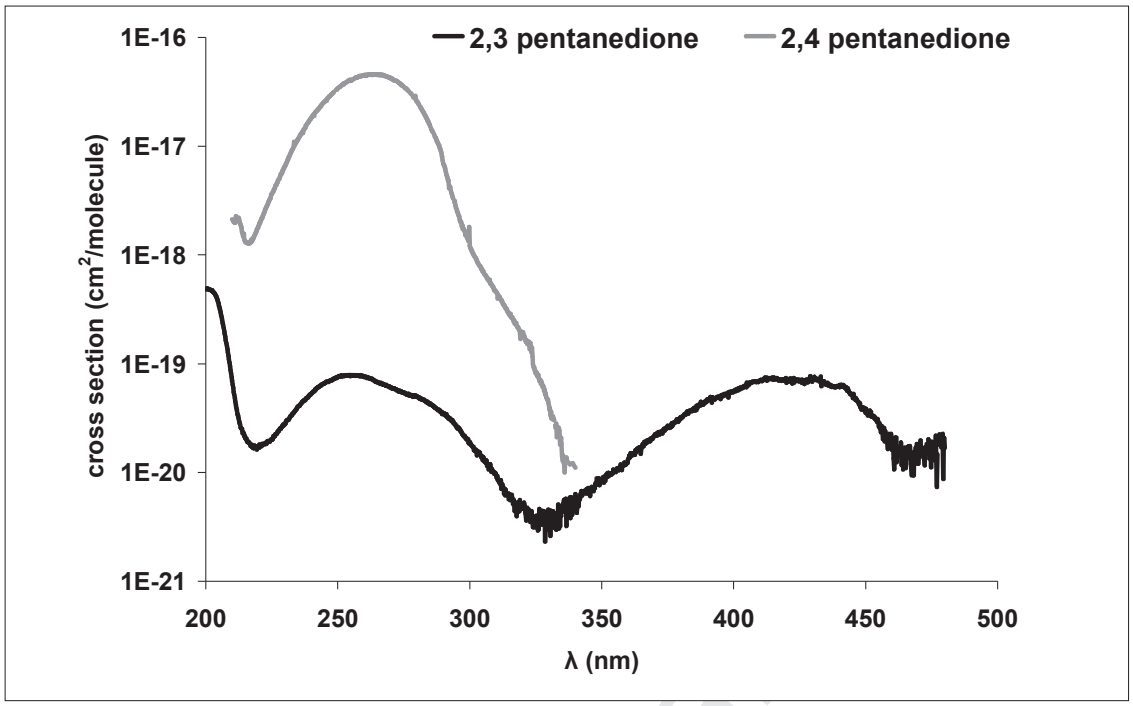

Figure 1. UV spectra obtained at 298 K for the two studied compounds.

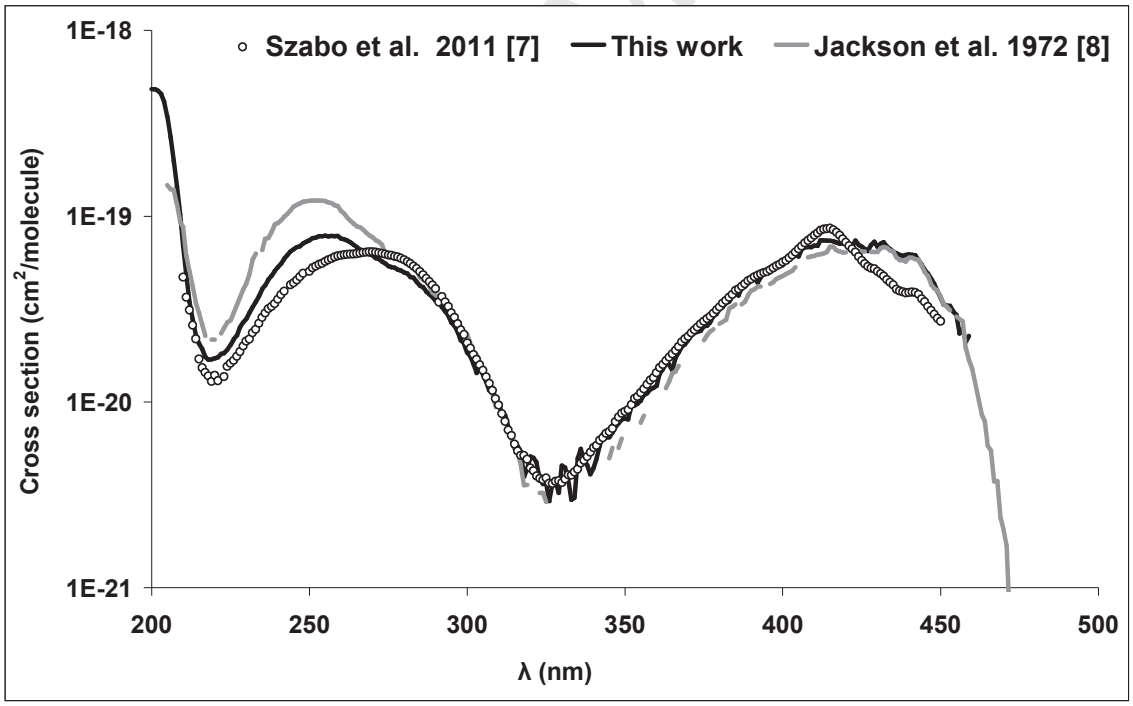

Figure 2: Comparison of the absorption cross sections of 2,3-pentanedione obtained in this work at 298 K with those found in the literature.

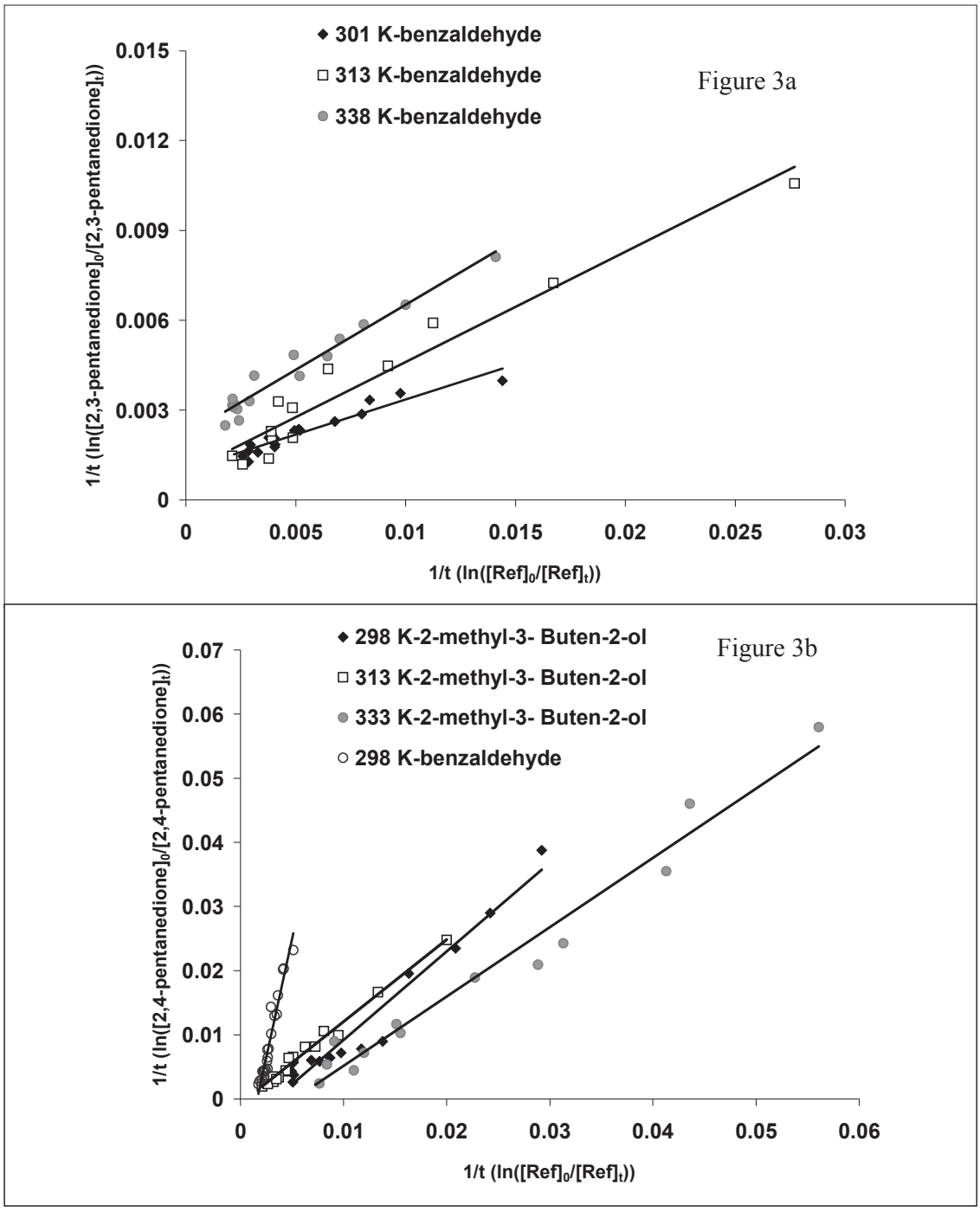

Figure 3: Relative rate plots for the reaction of OH with 2,3-pentanedione at different temperatures in the presence of benzaldehyde as reference compound (Figure 3a) and with 2,4-pentanedione at room temperature in the presence of benzaldehyde as reference compound and at different temperatures in the presence of 2-methyl-3-butene-2-ol as reference compound (Figure 3b).

Table 1 : Experimental conditions

The absorption cross sections measurements		
	2.3-pentanedione	**2.4-pentanedione**
P (Torr)	2.1 - 4	0.09 - 2
T (K)	298	298
Spectral range (nm)	210-460	210 - 340
Pathlength (cm)	50 -158	50 - 158
The kinetic study		
	2.3-pentanedione	**2.4-pentanedione**
Temperature (K)	301 - 338	298 - 333
Pressure (Torr)	600 - 760	600 - 760
Reference compound	benzaldehyde	benzaldehyde and 2-methyl-3- Buten-2-ol
Optical path (m)	24 - 32	24 - 32
[diketone] (ppm)	10 - 100	10 - 100
[Reference] (ppm)	10 - 100	10 - 100
Spectral range (cm^{-1}) (diketone)	1065.74 - 1009.3	810.10 - 728.17
Spectral range (cm^{-1}) (benzaldehyde)	2835 - 2765 2760 - 2700	2835 - 2765 2760 - 2700
Spectral range (cm^{-1}) (2-methyl-3-buten-2-ol)		3678.85 - 3602

Table 2: The UV Absorption cross-sections (σ : cm^2 $molecule^{-1}$) obtained for the studied compounds

2,3-pentanedione				2,4-pentanedione	
λ(nm)	$\sigma(10^{-20})$	λ(nm)	$\sigma(10^{-20})$	λ(nm)	$\sigma(10^{-18})$
200	48.37	331	0.44	210	2.13
201	48.35	332	0.39	211	1.98
202	47.31	333	0.30	212	2.15
203	45.50	334	0.31	213	1.97
204	41.45	335	0.49	214	1.54
205	34.49	336	0.56	215	1.32
206	26.74	337	0.49	216	1.28
207	19.86	338	0.46	217	1.30
208	14.51	339	0.41	218	1.41
209	10.23	340	0.44	219	1.61
210	6.96	341	0.49	220	1.85
211	4.84	342	0.58	221	2.11
212	3.46	343	0.67	222	2.42
213	2.80	344	0.64	223	2.75
214	2.29	345	0.65	224	3.13
215	2.06	346	0.69	225	3.63
216	1.93	347	0.73	226	4.06
217	1.75	348	0.77	227	4.59
218	1.69	349	0.81	228	5.16
219	1.70	350	0.82	229	5.86
220	1.72	351	0.81	230	6.58
221	1.74	352	0.96	231	7.46
222	1.82	353	0.96	232	8.41
223	1.83	354	0.98	233	9.54
224	1.91	355	1.02	234	10.57
225	2.03	356	1.09	235	11.69
226	2.18	357	1.12	236	12.86
227	2.28	358	1.17	237	14.09
228	2.52	359	1.19	238	15.48
229	2.69	360	1.22	239	16.86
230	2.80	361	1.41	240	18.22
231	3.03	362	1.50	241	18.99
232	3.25	363	1.60	242	21.05
233	3.47	364	1.59	243	22.52
234	3.73	365	1.48	244	24.11
235	4.06	366	1.73	245	25.73
236	4.25	367	1.85	246	27.32
237	4.56	368	1.99	247	28.78
238	4.77	369	2.04	248	30.56
239	5.07	370	2.15	249	32.32

240	5.32	371	2.28	250	33.92
241	5.55	372	2.36	251	35.43
242	5.91	373	2.39	252	36.74
243	6.17	374	2.42	253	38.33
244	6.45	375	2.55	254	39.99
245	6.62	376	2.57	255	40.18
246	6.82	377	2.69	256	41.57
247	6.90	378	2.89	257	42.74
248	7.14	379	2.98	258	43.92
249	7.29	380	3.19	259	44.16
250	7.43	381	3.25	260	45.02
251	7.61	382	3.40	261	45.30
252	7.68	383	3.47	262	45.91
253	7.79	384	3.72	263	45.57
254	7.79	385	3.84	264	45.50
255	7.88	386	3.75	265	45.47
256	7.77	387	4.14	266	45.11
257	7.83	388	4.17	267	45.03
258	7.80	389	4.35	268	44.14
259	7.83	390	4.52	269	43.52
260	7.59	391	4.69	270	42.35
261	7.51	392	4.39	271	40.66
262	7.39	393	4.68	272	40.32
263	7.24	394	4.95	273	38.64
264	7.01	395	4.93	274	36.99
265	6.82	396	5.19	275	34.81
266	6.61	397	5.17	276	33.80
267	6.50	398	5.37	277	31.94
268	6.37	399	5.51	278	29.99
269	6.25	400	5.46	279	27.89
270	6.16	401	5.60	280	25.70
271	5.95	402	5.94	281	24.09
272	5.88	403	6.02	282	21.43
273	5.69	404	6.22	283	19.33
274	5.57	405	6.08	284	17.32
275	5.40	406	6.62	285	15.06
276	5.33	407	6.79	286	13.57
277	5.28	408	6.83	287	12.10
278	5.15	409	6.82	288	10.59
279	5.10	410	6.97	289	9.13
280	4.98	411	6.93	290	6.89
281	4.92	412	7.43	291	5.75
282	4.71	413	7.41	292	4.85
283	4.66	414	7.40	293	3.76

284	4.43	415	7.37	294	3.27
285	4.24	416	7.35	295	2.63
286	4.15	417	7.25	296	2.26
287	3.93	418	7.12	297	1.84
288	3.80	419	7.15	298	1.69
289	3.67	420	7.38	299	1.44
290	3.51	421	6.85	300	1.21
291	3.43	422	6.88	301	1.07
292	3.24	423	7.39	302	0.96
293	3.08	424	7.00	303	0.86
294	2.92	425	6.89	304	0.78
295	2.68	426	6.68	305	0.71
296	2.57	427	6.50	306	0.65
297	2.37	428	7.00	307	0.59
298	2.15	429	7.30	308	0.55
299	2.07	430	6.85	309	0.50
300	1.85	431	7.12	310	0.46
301	1.76	432	7.25	311	0.42
302	1.60	433	6.88	312	0.38
303	1.43	434	6.66	313	0.35
304	1.52	435	6.45	314	0.32
305	1.40	436	6.32	315	0.28
306	1.28	437	6.18	316	0.26
307	1.16	438	6.13	317	0.24
308	1.19	439	6.18	318	0.22
309	1.03	440	6.24	319	0.20
310	0.98	441	6.20	320	0.18
311	0.87	442	6.17	321	0.17
312	0.85	443	5.84	322	0.16
313	0.73	444	5.48	323	0.15
314	0.64	445	5.14	324	0.10
315	0.57	446	4.92	325	0.08
316	0.58	447	4.60	326	0.08
317	0.54	448	4.33	327	0.07
318	0.40	449	3.97	328	0.06
319	0.44	450	3.66	329	0.05
320	0.51	451	3.35	330	0.04
321	0.50	452	3.31	331	0.03
322	0.47	453	3.29	332	0.03
323	0.39	454	3.07	333	0.02
324	0.36	455	2.95	334	0.02
325	0.36	456	2.34	335	0.01
326	0.29	457	2.48	336	0.01
327	0.36	458	2.11	337	0.01

328	0.38	459	2.27	338	0.01
329	0.32	460	1.63	339	0.01
330	0.45	461	1.07	340	0.01

Table 3: The average rate coefficients for the reactions of the studied diketones with OH

	Reference	Temperature (K)	k/kref	k (cm^3 $molecule^{-1}$ s^{-1})
2.3-pentanedione + OH	Benzaldehyde	301	0.27 ± 0.04	(3.23± 0.80) $\times 10^{-12}$
		318	0.34 ± 0.03	(3.89± 0.90) $\times 10^{-12}$
		338	0.42 ± 0.04	(4.52± 1.00) $\times 10^{-12}$
2.4-pentanedione + OH	2-methyl -3-butène-2-ol	298	1.38 ± 0.20	(8.76± 2.70) $\times 10^{-11}$
		313	1.31± 0.12	(7.54± 2.30) $\times 10^{-11}$
		338	1.23± 0.15	(6.30± 1.90) $\times 10^{-11}$
	Benzaldehyde	298	7.40± 0.40	(8.89±0.80.) $\times 10^{-11}$

Table 4: Photodissociation rate constants J_p (upper limits) as a function of solar zenith angle

Compound	Photodissociation rate constants $J_p(s^{-1})$			
	θ =20°	θ =30°	θ =40°	θ =50°
2.3-pentanedione	5.50×10^{-5}	5.28×10^{-5}	4.96×10^{-5}	4.42×10^{-5}
2.4-pentanedione	4.33×10^{-4}	3.86×10^{-4}	3.21×10^{-4}	2.40×10^{-4}

Table 5: Tropospheric lifetimes (in days) of 2,3-pentanedione and 2,4-pentanedione due to photolysis and their gas phase reactions with atmospheric photooxidants.

Compound	$\tau_{photolysis}$ [a]	τ_{OH} [b]	τ_{O3} [c]	τ_{Cl} [d]
2,3- pentanedione	> 5 h	3.6 days	/	82.6 days
2,4- pentanedione	> 43 min	3 hours	16.1 days	/

[a] calculated by using the photolysis rates for a solar zenith angle of 30°.

[b] calculated in this work using a OH 24-h average concentration of 1×10^6 molecules cm^{-3} reported by Atkinson et al., [28] and the rate coefficient determined in the present work

[c] reported by Zhou et al. [11]

[d] calculated by using the rate constant reported by Kaiser et al., [3] work with an upper limit of 1×10^3 molecule cm^{-3} for Cl concentration reported by Wingenter et al., [29].